higher L/r values, Brazier flattening (which tends to be imperfection insensitive) is accentuated and agreement with the design criteria correlated with experiment is better.

References

[1] Brazier, L. G., "On the Flexure of Thin Cylindrical Shells and Other 'Thin' Sections," *Proceedings of the Royal Society, Series A*, Vol. CXVI, 1926, pp. 104–114.

[2] Seide, P., and Weingarten, V. I., "On the Buckling of Circular Cylindrical Shells Under Pure Bending," *Journal of Applied Mechanics*, Vol. 28, 1961, pp. 112–116.

[3] Aksel'rad, E. L., "Refinement of the Upper Critical Loading of Pipe Bending Taking Account of the Geometrical Nonlinearity" (in Russian), *Izvestiia, AN, SSSR, OTN, Mekhanika i Mashinostroenie*, No. 4, 1965, pp. 123–139.

[4] Almroth, B. O., and Starnes, James H., Jr., "The Computer in Shell Stability Analysis," *presented at the 1973 ASCE National Structural Engineering Meeting*, San Francisco, Calif., April 9–13, 1973.

[5] Almroth, B. O., Brogan, F. A., and Marlowe, M. B., "Collapse Analysis for Shells of General Shape," *Vol. I: Analysis*, AFFDL–TR–71–8, Aug. 1972, Air Force Flight Dynamics Lab., Wright-Patterson Air Force Base, Ohio.

[6] Almroth, B. O., Brogan, F. A., Meller, E., Zele, F., and Peterson, H. T., "Collapse Analysis for Shells of General Shape, Vol. II, User's Manual for the STAGS-A Computer Code," AFFDL–TR–71–8, March 1973.

[7] *Buckling of Thin-Walled Circular Cylinders*, SP–8007, Aug. 1968, NASA.

[8] Baker, E. H., Cappelli, A. P., Kovalevsky, L., Rish, F. L., and Verette, R. M., "Shell Analysis Manual," CR–912, April 1968, NASA.

[9] Sobel, L. H., "Effects of Boundary Conditions on the Stability of Cylinders Subject to Lateral and Axial Pressures," *AIAA Journal*, Vol. 2, No. 8, Aug. 1964, pp. 1437–1440.

JANUARY 1975 AIAA JOURNAL VOL. 13, NO. 1

Nonstationary Spectral Analysis for Linear Dynamic Systems

W. R. DAVIS JR.*
Air Force Flight Dynamics Laboratory, Wright-Patterson Air Force Base, Ohio
AND
L. L. BUCCIARELLI JR.†
Smithsonian Institution, Washington, D.C.

Second-order statistics of nonstationary processes in the form of time dependent spectra are studied with emphasis on "instantaneous" and "evolutionary" spectral densities. An integrated procedure for the time dependent spectral response calculation for linear systems with digital analysis of input data is presented for excitation processes in the form of a product of a deterministic envelope and a stationary random process. The envelope is approximated using a finite sum Fourier series, the Fourier coefficients being estimated directly from input time records. An example, using artificial earthquake motions, illustrates the procedure.

Nomenclature

$A(t, \omega)$ = envelope function [see Eq. (11)]
a_m = Fourier coefficient of $c(t)$
b = bias error
$c(t)$ = envelope function [see Eq. (1)]
c_m = measured Fourier coefficient of $c(t)$
$d(t)$ = measured estimate of $c(t)$
$f_y(t, \omega)$ = evolutionary spectral density of process y
$H(\omega)$ = Fourier transform of $h(t)$
$h(t)$ = impulse response of time invariant linear system
i = $(-1)^{1/2}$
M = number of sampled points in discrete Fourier transform
N = number of realizations in experimental average
$n(t)$ = stationary random process
R = order of Fourier series approximation
$R_n(t)$ = autocorrelation of process n
$\hat{R}_n(t)$ = normalized autocorrelation [see Eq. (29)]
r = frequency resolution parameter [see Eq. (33)]
$S_n(\omega)$ = spectral density of process n
T = Fourier series period
T_1 = see Fig. (5)
$\bar{T}$ = nonzero range of $c(t)$
$X(\omega)$ = Fourier transform of $x(t)$
$x(t)$ = nonstationary excitation process
$y(t)$ = nonstationary linear system response process
$\langle \ldots \rangle$ = ensemble average
α = see Eq. (16)
Δf = frequency increment
Δt = time increment
ε = total error in estimation of $c(t)$
ζ = damping ratio
μ = see Eq. (29)
ν = variability error
σ_n = standard deviation of process n
$\Phi_x(t, \omega)$ = instantaneous spectral density
$\phi_x(t, \tau)$ = nonstationary autocorrelation [see Eq. (6)]
ω_d = damped natural frequency
ω_n = natural frequency
ω_0 = see Eq. (16)
$\hat{\omega}$ = see Eq. (2)

Superscripts
$*$ = complex conjugate

Subscripts
p = periodic version
R = order of Fourier series approximation

Presented as Paper 74-137 at the AIAA 12th Aerospace Sciences Meeting, Washington, D.C., January 30–February 1, 1974; submitted February 19, 1974; revision received July 1, 1974. This research was supported by the MIT Lincoln Laboratory under sponsorship of the U.S. Air Force.

Index category: Structural Dynamic Analysis.

* Aerospace Engineer, Vehicle Dynamics Division. Associate Member AIAA.

† Curator, Department of Science and Technology, National Air and Space Museum.

Introduction

RECENTLY, important problems in random vibration have emerged for which stationary analysis is inadequate and more complicated nonstationary methods are required. Examples include the design of buildings for earthquake survivability, the response of aircraft to atmospheric turbulence, and the response of spacecraft to pyrotechnic shock. Several researchers have calculated mean square response of linear systems for special cases of nonstationary input.[1-4] However, in some cases mean square response supplies insufficient information, and higher order statistics of response must be considered.

Second-order statistics are most commonly expressed in terms of the nonstationary autocorrelation function. Linear response relations for the autocorrelation involve double time domain integrals which may be difficult or time consuming to evaluate. The autocorrelation also may be difficult to measure experimentally, requiring time pair analysis and ensemble average operations. Recently, researchers have extended the more physically meaningful concept of spectral density to nonstationary processes by defining spectra dependent on both time and frequency and which contain stationary spectral analysis as a special case.[5-8] Several authors have used an "evolutionary spectrum" for linear response calculations.[9,10,21]

The object of this paper is to consider some of the advantages of time dependent spectral representations and to present a new integrated procedure for the approximate calculation of linear system response with a method for measuring input parameters directly from experimental excitation records. The technique offers advantages over previous methods in terms of computational effort, and special consideration is given to practical applications.

Excitation processes are restricted to the form

$$x(t) = c(t)n(t) \tag{1}$$

where $c(t)$ is a positive, real-valued, deterministic envelope which is pulselike or non-zero only over a finite range; and $n(t)$ is a zero mean, stationary, normally distributed, random process.

To develop approximate input-output relations for "instantaneous" and "evolutionary" spectra for inputs given by Eq. (1), we approximate $c(t)$ by a finite sum Fourier series as Roberts[11,12] has done in estimating the autocorrelation response of linear systems. A pulse-like envelope $c(t)$, nonzero only in the range $(0, \bar{T})$, has a Fourier series representation valid in the range $(0, T)$ and periodic with period T:

$$c(t) = \sum_{m=-\infty}^{+\infty} a_m e^{im\hat{\omega}t} \qquad 0 \leqq t \leqq T \tag{2}$$

where $\hat{\omega} = 2\pi/T$ and

$$a_m = \frac{1}{T}\int_0^{\bar{T}} c(t)\, e^{-im\hat{\omega}t} \qquad \bar{T} < T \tag{3}$$

We might approximate $c(t)$ using a finite sum series.

$$c(t) \cong \sum_{m=-R}^{+R} a_m e^{im\hat{\omega}t} \qquad 0 \leqq t \leqq T \tag{4}$$

If $c(t)$ is slowly varying, and the series is convergent, we expect a good approximation for small values of R.

Instantaneous and Evolutionary Spectra

The "instantaneous" spectrum, $\Phi_x(t, \omega)$, for a process $x(t)$ as developed by Mark[8] is defined as the Fourier transform of an autocorrelation $\phi_x(t, \tau)$

$$\Phi_x(t, \omega) = \int_{-\infty}^{+\infty} \phi_x(t, \tau) e^{-i\omega\tau}\, d\tau \tag{5}$$

where $\phi_x(t, \tau)$ is taken as

$$\phi_x(t, \tau) = \langle x(t+\tau/2)x(t-\tau/2)\rangle \tag{6}$$

$\phi_x(t, \tau)$ is an even function of τ to insure $\Phi_x(t, \omega)$ is real.

Mark formulates a linear response relation using the symmetric function

$$\Phi_h(t, \omega) = \int_{-\infty}^{+\infty} h(t+\tau/2)h(t-\tau/2)\, e^{i\omega\tau}\, d\tau = \frac{1}{2\pi}\int_{-\infty}^{\infty} H(\omega - v/2)H^*(\omega + v/2)\, e^{-ivt}\, dv \tag{7}$$

He obtains the instanteous spectral density of the response variable, $y(t)$, for an excitation, $x(t)$, in terms of a simple convolution:

$$\Phi_y(t, \omega) = \int_{-\infty}^{+\infty} \Phi_h(t-\bar{t}, \omega)\Phi_x(\bar{t}, \omega)\, d\bar{t} \tag{8}$$

We now consider the possibility of replacing $c(t)$, in the excitation $x(t) = c(t)n(t)$, with an infinite train of pulses represented by Eq. (2). If the linear system is damped and the spacing between pulses, $T - \bar{T}$, is large enough, then the response, $y(t)$, will decay to a negligible value between pulses; and $y(t)$ will be very close to the response to an isolated pulse. We find

$$\Phi_x(t, \omega) = \sum_{m=-\infty}^{+\infty} \sum_{k=-\infty}^{+\infty} a_m a_k^*\, e^{i\hat{\omega}(m-k)t} \times S_n[\omega - (m\hat{\omega}/2) - (k\hat{\omega}/2)] \tag{9}$$

The approximate linear response relation is obtained by performing the integration of Eq. (8) using Eqs. (7) and (9). Since we have a representation for $c(t)$ over the infinite time domain, we are able to reduce the result to

$$\Phi_y(t, \omega) = \sum_{m=-\infty}^{+\infty} \sum_{k=-\infty}^{+\infty} a_m a_k^* S_n[\omega - (m+k)\hat{\omega}/2] \times \times e^{i(k-m)\hat{\omega}t} H[\omega - (m-k)\hat{\omega}/2]H^*[\omega + (m-k)\hat{\omega}/2] \tag{10}$$

using generalized functions.

The "evolutionary" spectrum, as developed by Priestley,[6-7] depends on a generalized harmonic analysis representation for a process $x(t)$ given by

$$x(t) = \frac{1}{2\pi}\int_{-\infty}^{+\infty} A(t, \omega)\, e^{i\omega t}\, dX(\omega) \tag{11}$$

which Priestley claims is valid for a large class of nonstationary processes.

The evolutionary spectrum takes a special form when $x(t)$ is a "uniformly modulated process," i.e., in the form of Eq. (1) with $c(t)$ an oscillatory function, a condition satisfied by non-negative, real-valued functions whose Fourier transforms exist.[6] The resulting spectrum always separates in time and frequency,

$$f_x(t, \omega) = |c(t)|^2 S_n(\omega) \tag{12}$$

unlike the instantaneous spectrum.

Following Shinozuka,[13] the linear response relation for an excitation described by Eq. (11) is

$$f_y(t, \omega) = \left|\int_{-\infty}^{+\infty} A(\tau, \omega)h(t-\tau)\, e^{i\omega\tau}\, d\tau\right|^2 S_x(\omega) \tag{13}$$

For a uniformly modulated process, $c(\tau)$ replaces $A(\tau, \omega)$ and $S_n(\omega)$ replaces $S_x(\omega)$.

Taking a Fourier series approximation for $c(t)$ and noting that we require $c(t)$ only for the times of interest, we simply use Eq. (2) in the range $(0, T)$ without the need for a train of pulses. Combining Eqs. (2) and (13) with $A(\tau, \omega)$ replaced by $c(\tau)$, we find

$$f_y(t, \omega) = \left|\sum_{m=-\infty}^{+\infty} a_m e^{im\hat{\omega}t} \times \int_0^t h(\tau)\, e^{-i(\omega + m\hat{\omega})\tau}\, d\tau\right|^2 S_n(\omega) \qquad 0 \leqq t \leqq T \tag{14}$$

In comparing the instantaneous and evolutionary formulations, we note that Eq. (14) differs from Eq. (10) in several important ways. The former has only a single sum over the Fourier coefficients, while the latter requires a double sum. Also zero initial conditions for the evolutionary result are always satisfied, while initial conditions depend on pulse separation for the instantaneous result. Both the instantaneous and evolutionary spectra have interpretations as energy densities, since the mean-square value of a given process is obtained from an integral

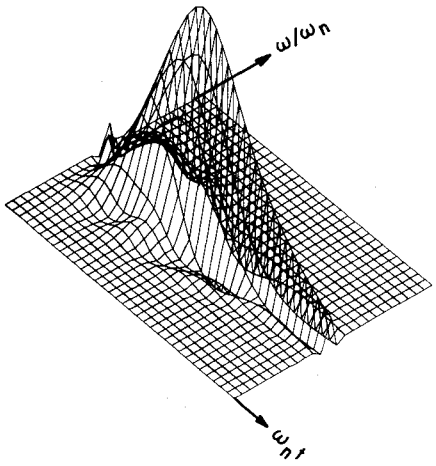

Fig. 1 Instantaneous spectral density of response for rectangular step envelope. $R = 5$, $T = 3\bar{T}$. **Range of variables:** $\omega/\omega_n = (0.87, 1.12)$; $\omega_n t = (0, 300)$.

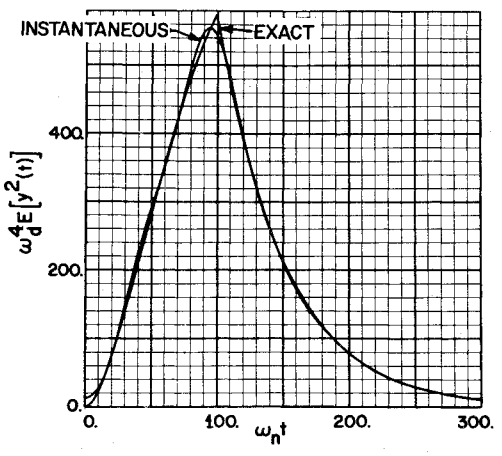

Fig. 3 Instantaneous and exact mean square responses for rectangular step envelope. $R = 5$, $T = 3\bar{T}$.

in frequency over the pertinent spectrum. Note, however, that the instantaneous spectrum may be negative while the evolutionary definition is always positive. A very important characteristic of the evolutionary spectrum is that its moments can be related directly to first passage probabilities and other statistical measures for Gaussian random processes.[14-16]

Mark and Priestley present experimental techniques for measuring time-dependent spectra which are similar. Both require two-dimensional time and frequency domain filtering which is governed by an "uncertainty principle,"[6-8] establishing the interdependence of frequency and time resolution. The time-dependent spectra appear to offer advantages over the auto-correlation representation including simpler linear response relations, ease of measurement, and physical significance. We use the instantaneous and evolutionary spectra in the following development of an integrated procedure for data analysis and linear response approximation.

An Example

We now consider the use of Rth order finite sums in Eqs. (10) and (14) to approximate the spectra. It is desirable to test the accuracy of these approximations; unfortunately exact results for time-dependent spectra are not readily available. However, Barnoski and Maurer[2] present exact results for mean square response to several simple nonstationary inputs. Mean square response is obtained from $\Phi_y(t, \omega)$ and $f_y(t, \omega)$ by integration over ω and used as a basis for comparison.

For our example we use a rectangular step for $c(t)$, i.e.,

$$\begin{aligned} c(t) &= 1 \qquad 0 \leqq t \leqq \bar{T} \\ &= 0 \qquad \text{otherwise} \end{aligned} \tag{15}$$

and $n(t)$ is narrow-band random noise with

$$R_n(\tau) = e^{-\alpha|\tau|}\cos\omega_0\tau \tag{16}$$

Our linear system is

$$\ddot{y}(t) + 2\zeta\omega_n\dot{y}(t) + \omega_n^2 y(t) = x(t) \tag{17}$$

where a dot represents differentiation with respect to time.

Equations (10) and (14) are solved digitally for the parameters $\zeta = 0.01, \alpha/\zeta\omega_n = 2$, $\omega_n\bar{T} = 100$, $T = 3\bar{T}$, and $\omega_d/\omega_0 = 1$ using 100 time increments and 50 frequency increments over the range $\omega/\omega_n = (0.75, 1.25)$. Note $\omega_d = (1-\zeta^2)^{1/2}\omega_n$. Sections of the resulting spectra are plotted in three-dimensional form in Figs. 1 and 2 for 5th-order Fourier approximation ($R = 5$). Negative value spurious behavior is obvious in the instantaneous result, while the evolutionary spectrum is smooth and positive. The resulting mean square responses are plotted in Figs. 3 and 4 together with the exact results.[2] We see acceptable accuracy is obtainable even for small values of R. Instantaneous spectrum results are calculated only for $R = 5$ because of the excessive computer time required to perform the double sum in Eq. (10). We should note that, if we decrease the ratio $T/\bar{T}$, the accuracy of the instantaneous result would decrease and the response at zero time would move further away from zero, since we are considering the response to a train of pulses.

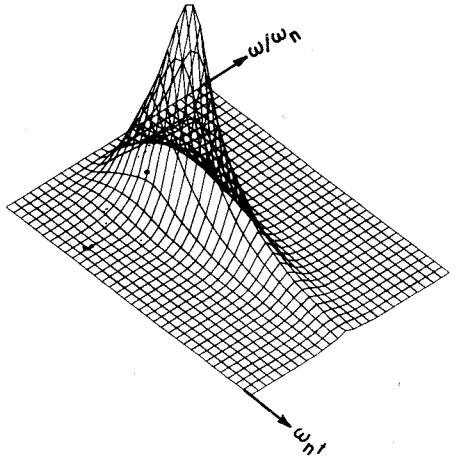

Fig. 2 Evolutionary spectral density of response for rectangular step envelope. $R = 5$, $T = 3\bar{T}$. **Range of variables:** $\omega/\omega_n = (0.87, 1.12)$; $\omega_n t = (0, 300)$.

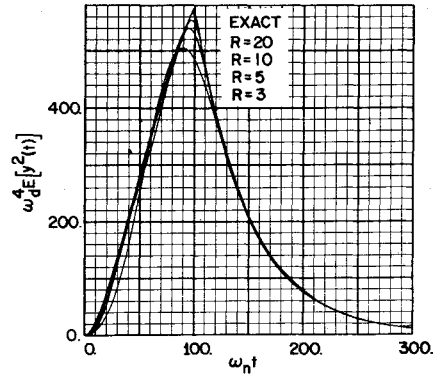

Fig. 4 Evolutionary and exact mean square responses for rectangular step envelope. $R = 3, 5, 10, 20$; $T = 3\bar{T}$.

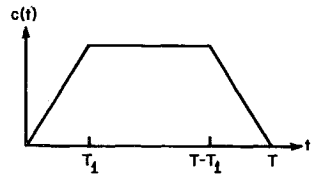

Fig. 5 Envelope function $c(t)$.

It is instructive to compare the approximate evolutionary spectrum solution given by Eq. (14) with direct numerical integration of Eq. (13). Although computational times for equivalent accuracy are comparable for the previous example, care should be taken in comparing results. At a given time instant the accuracy of the Fourier response approximation depends only on R and is independent of the time increment size, while the accuracy of the direct integration is entirely dependent on the time increment and the response at all previous times. We now consider a technique for estimating the Fourier coefficients of $c(t)$ directly from experimental data.

Fourier Coefficient Estimation

Roberts[17] suggests a method of smoothing estimates of the mean square value of nonstationary processes with finite Fourier series. He computes an expression for the integrated mean square error associated with the smoothing and shows that it can increase the accuracy of the mean square estimation.

Here a procedure similar to Roberts' is presented for estimating the coefficients of $c(t)$ from the Fourier smoothing of the absolute value of uniformly modulated processes when $n(t)$ has a Gaussian distribution. The absolute value is used instead of the square since the latter leads to Fourier coefficients of $c^2(t)$ while the coefficients of $c(t)$ are required for the linear response relations. Also, the absolute value is less time-consuming to compute digitally. A calculation of the integrated mean square error in the measurement is included.

Taking the absolute value of Eq. (1) and forming the ensemble average, we find

$$\langle|x(t)|\rangle = c(t)\langle|n(t)|\rangle \tag{18}$$

In Ref. 18 it is shown that the first absolute moment of $n(t)$ is proportional to σ_n. Using this we may rearrange Eq. (18) to form an expression for $c(t)$:

$$c(t) = (\pi/2)^{1/2}\langle|x(t)|\rangle/\sigma_n \tag{19}$$

We define a new process $d(t)$, which is an experimentally measurable estimate of $c(t)$, as an ensemble average of N records of $x(t)$:

$$d(t) \equiv \frac{(\pi/2)^{1/2}}{\sigma_n N}\sum_{j=1}^{N}|x_j(t)| \tag{20}$$

Taking the expected value of Eq. (20), we find

$$\langle d(t)\rangle = c(t) \tag{21}$$

and $d(t)$ is therefore an unbiased estimate of $c(t)$. We propose to smooth $d(t)$ using a finite sum Fourier series. $d(t)$ has a Fourier series representation

$$d(t) = \sum_{m=-\infty}^{+\infty} c_m e^{im\hat{\omega}t} \qquad 0 \leq t \leq T \tag{22}$$

where

$$c_m = \frac{1}{T}\int_0^T d(t)e^{-im\hat{\omega}t}\,dt \tag{23}$$

We have

$$\langle c_m\rangle = a_m \tag{24}$$

so the c_m are unbiased estimates of the a_m; and we may estimate the a_m by performing the operation of Eq. (23) on experimental records.

A smoothed version of $d(t)$, $d_R(t)$, is formed by taking R terms in the sum of Eq. (22). We want to choose R small enough to smooth local variations in $d(t)$ but large enough to estimate $c(t)$ with sufficient accuracy.

Table 1 Bias error

R	Bias error, b $T_1/T = 0.1$	$T_1/T = 0.25$	$T_1/T = 0.5$
0	0.05667	0.10417	0.08333
1	0.03794	0.02204	0.00121
2	0.02263	0.00151	0.00121
3	0.01177	0.00049	0.00019
4	0.00521	0.00049	0.00019
5	0.00192	0.00036	0.00006

To aid in the selection of optimum R, we consider the integrated mean square error ε as a measure of the average discrepancy between $c(t)$ and the smoothed estimate $d_R(t)$,

$$\varepsilon = \frac{1}{T}\int_0^T \langle[d_R(t)-c(t)]^2\rangle\,dt = b+v \tag{25}$$

The first term, b, is called the bias error, and the second, v, is the variability. We find

$$b = \frac{1}{T}\int_0^T c^2(t)\,dt - \sum_{m=-R}^{+R}|a_m|^2 \tag{26}$$

which is simply the error in approximating $c(t)$ with a finite sum Fourier series. b is independent of N and the statistics of $n(t)$.

The variability error may be written in terms of the Fourier coefficients as

$$v = \sum_{m=-R}^{+R}[\langle|c_m|^2\rangle - |a_m|^2] \tag{27}$$

If we assume different experimental realizations of $x(t)$ are uncorrelated and that $n(t)$ is a Gaussian random process, we may show[19]

$$v = \frac{1}{NT^2}\sum_{m=-R}^{+R}\int_0^T\int_0^T c(t_1)c(t_2)[\cos\mu + \mu\sin\mu - 1]\times e^{-im\hat{\omega}(t_1-t_2)}\,dt_1\,dt_2 \tag{28}$$

where

$$\sin\mu = R_n(t_1-t_2)/\sigma_n^2 \equiv \hat{R}_n(t_1-t_2) \tag{29}$$

So the variability is inversely proportional to N, the number of experimental records, and depends on the second order statistics of $n(t)$ through the function μ.

To study the behavior of the mean square error empirically, we consider an example where $n(t)$ is an ideal bandpass process and $c(t)$ is a trapezoidal pulse. $n(t)$ is described by its autocorrelation,

$$R_n(\tau) = [\sin\omega_u\tau - \sin\omega_l\tau]/(\omega_u-\omega_l)\tau \tag{30}$$

where ω_u and ω_l are upper and lower cutoff frequencies. $c(t)$ is shown in Fig. 5 where T_1/T is used as a measure of the "rise

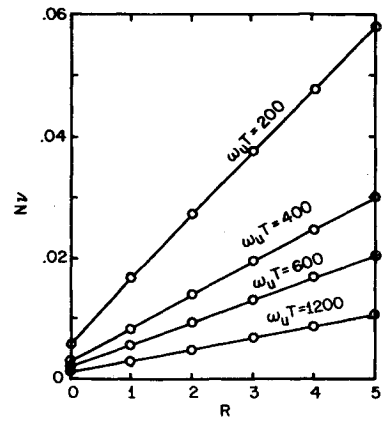

Fig. 6 Effect of bandwidth on variability error. $\omega_l T = 0$, $T_1/T = 0.25$.

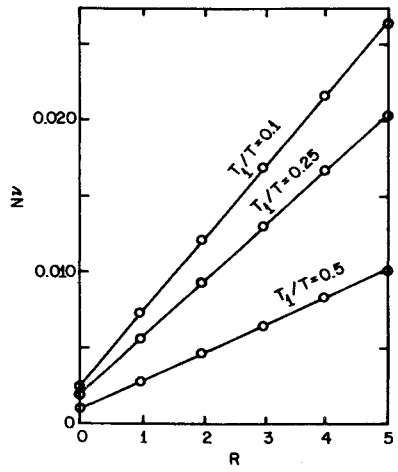

Fig. 7 Effect of pulse rise time on variability error. $\omega_l T = 0$, $\omega_u T = 600$.

time" of the pulse. We study the behavior of the error as T_1/T, R, and the bandwidth of $n(t)$ are varied. b is calculated directly from Eq. (26), while v is found from a trapezoid rule solution of Eq. (28).

The bias error depends on R and T_1/T but is independent of bandwidth. From Table 1 we see that the bias decreases as R increases, decreasing more rapidly as rise time increases.

The behavior of the variability error is illustrated in Figs. 6 and 7. In Fig. 6 bandwidth is varied with rise time constant, while in the second the converse situation is shown. The error exists only at integer values of R: data points are connected with straight lines merely for clarity. In both cases the variability increases monotonically with R. This is expected since $d_R(t)$ has a greater tendency to follow rapidly varying local variations in $d(t)$ as R is increased. In Fig. 6, v decreases as bandwidth increases for a given value of R. In this case as ω_u increases while the average power of $n(t)$ remains constant, the local variations become spread out over a broader and higher frequency range so that at a given R there is greater tendency to smooth $d(t)$. In Fig. 7 error increases as the pulse rise time decreases for a given value of R. This is plausible since the more rapidly the envelope varies, the more difficult it is to separate the envelope shape from local variations in $d_R(t)$.

Since the bias decreases with increasing R, while the variability increases, we expect to find a minimum at a particular value of R when the two are summed to form the total error ε. This is confirmed for this example in Fig. 8 where total error is plotted for several values of N.

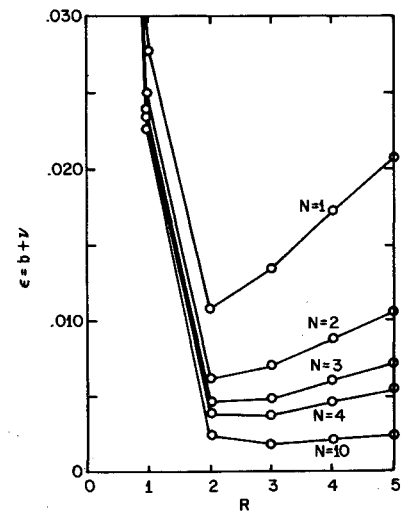

Fig. 8 Variation of total error with number of ensemble members. $\omega_l T = 0$, $\omega_u T = 600$, $T_1/T = 0.25$.

In summary, for our representative example the mean square error achieves an optimum at a particular value of R, this value depending on the bandwidth of the measured process, the rise time of the envelope pulse, and the number of realizations in the ensemble average. Since we have a technique for measuring the Fourier coefficients of $c(t)$, we consider the estimation of $S_n(\omega)$, the other input parameter required for the linear response relations.

Spectral Density Estimation

We propose to estimate $S_n(\omega)$ experimentally from an ensemble average of the squared Fourier transform moduli of records from the excitation process $x(t) = c(t)n(t)$. In Ref. 19 the Fourier coefficients of $c(t)$ are used in the determination of bounds on $S_n(\omega)$, the tightness of which depend on the characteristics of the coefficients. To take advantage of the fast Fourier transform (FFT) algorithm, the procedure is derived in terms of finite discrete transforms.

If $x(t)$ is sampled at M points with increment Δt, the discrete Fourier transform considers $x(t)$ to be periodic with period $T = M\Delta t$ and returns a periodic frequency domain transform with period $F = 1/\Delta t$ and frequency increment $\Delta f = 1/T$. The frequency domain transform is

$$X_p(k\Delta f) = \Delta t \sum_{j=0}^{M-1} x_p(j\Delta t)\, e^{-(2\pi i)jk/M} \approx X(k\Delta f) \qquad |k\Delta f| \leqq F/2 \tag{31}$$

assuming Δt is small enough to prevent aliasing. In Ref. 19, we obtain

$$\langle X_p(f)X_p^*(f)\rangle = T \sum_{m=-M/2}^{+M/2} |a_m|^2 S_{n_p}(f - m/T) \tag{32}$$

Now we would like to take

$$S_n(f) \cong \langle X_p(f)X_p^*(f)\rangle/T \sum_{m=-r}^{+r} |a_m|^2 \tag{33}$$

as an estimation of $S_n(f)$. Evidently, if $S_{n_p}(f)$ is sufficiently smooth so that a frequency shift of r/T has negligible effect, then

$$S_{n_p}(f - m/T) \cong S_{n_p}(f) \qquad |m| \leqq r \tag{34}$$

Note also that if $c(t)$ is relatively slowly varying, the Fourier coefficients a_m decay rapidly as $|m|$ increases and $\langle X_p X_p^*\rangle$ is a summation over $S_{n_p}(f)$ evaluated at slightly different frequencies in which case Eq. (33) is reasonable. In fact, we may show[19] that the right-hand side of Eq. (33) is an upper bound on $S_n(f)$.

A lower bound has also been obtained which depends on the smoothness of $S_n(f)$ and the time varying character of $c(t)$, that is, for a given value of r the "tightness" of these bounds formed depends on how rapidly a_m decreases as $|m|$ increases; thus the more slowly $c(t)$ varies, the tighter the bound.

In practice we estimate $\langle X_p(f)X_p^*(f)\rangle$ by taking discrete Fourier transforms of a finite number of experimental records of $x(t)$ and averaging their moduli to approximate the ensemble average. Fourier coefficients of $c(t)$ may be estimated using the techniques of the previous section.

Example of Integrated Analysis Procedure

As an example of the incorporation of the previous techniques into an integrated procedure for data analysis and response approximation, we consider an ensemble of four artificially constructed earthquake motions.‡

The time histories are in the form of Eq. (1) where $c(t)$ is the trapezoidal pulse given in Fig. 5 with $T = 20$ sec and $T_1 = 5$ sec. We may assume each record is a realization of the same random process with $n(t)$ being normally distributed and $S_n(\omega)$ having

‡ Earthquake time histories were supplied by E. H. Vanmarcke of the Department of Civil Engineering, MIT, Cambridge, Mass.

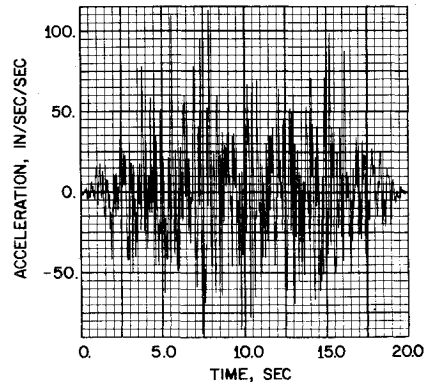

Fig. 9 Artificial earthquake motion—example time history.

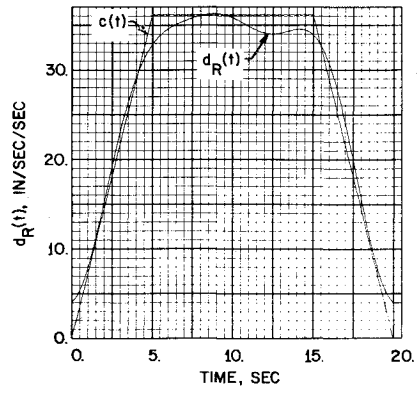

Fig. 12 Fourier smoothed estimate of $c(t)$. $R = 3$.

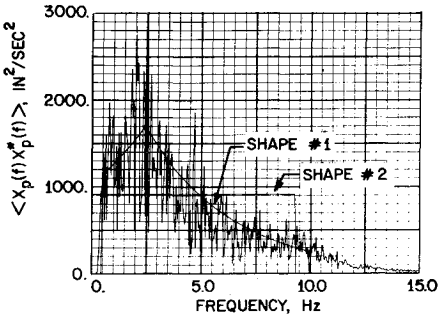

Fig. 10 Assumed shapes for $S_n(f)$.

the shape of exponentially decaying functions with a peak at 2.5 Hz.[20] An example time history is shown in Fig. 9.

We begin by computing the discrete Fourier transform of each record since the time step size and record length must be chosen to prevent aliasing and provide adequate frequency resolution. By using the FFT algorithm with $\Delta t = 0.01$ sec, $\Delta f = 0.0488$ Hz, $M = 2048$, and a Nyquist frequency of 50 Hz, the transform moduli are computed and then added and divided by four to approximate $\langle X_p(f)X_p^*(f)\rangle$. This result is plotted in Fig. 10 for the range in which there is significant contribution.

Next we perform an average over the four realizations of $x(t)$ to approximate $\langle|x(t)|\rangle$: the result is shown in Fig. 11. The trapezoidal pulse shape is apparent even with only four records in the average. Forming $d(t)$ [Eq. (20)] and using a trapezoid rule approximation of Eq. (23), we calculate the estimated coefficients, c_m. To illustrate the smoothing effect of the finite sum series, we may calculate $d_R(t)$ using the c_m. The $R = 3$ case is shown in Fig. 12.

To select the optimum order of smoothing, we consider the bias and variability errors. The bias, Eq. (26), depends on $c(t)$ and the a_m, while the variability, Eq. (28), depends on $c(t)$ and $\hat{R}_n(t)$. These quantities are known for this example, but we might consider what results are obtainable if the process were unknown, i.e., using the c_m in place of the a_m, and estimating $c(t)$ and $\hat{R}_n(\tau)$.

The variability depends on $\hat{R}_n(t)$ which is in turn related to $S_n(\omega)$, but only the shape of $S_n(\omega)$ is required since $\hat{R}_n(t)$ is normalized as in Eq. (29). Assuming $\langle X_p(f)X_p^*(f)\rangle$ and $S_n(\omega)$ have the same shape, we choose the exponentially decaying curve labeled Shape No. 1 in Fig. 10. If we take the Fourier transform of this shape, normalize, and apply the result to a trapezoid rule solution of Eq. (28), we obtain v, which is plotted as a solid line in Fig. 13.

To gage the dependence of the variability on the choice of $S_n(\omega)$ we consider the curve labeled Shape No. 2 in Fig. 10 which has the same integrated area as Shape No. 1. The resulting variability is plotted as a dashed line in Fig. 13 and is very close to the previous result, indicating that this measure of error is insensitive to the assumed shape of $S_n(\omega)$. The total error, $(\varepsilon = b + v)$, is plotted in Fig. 14 based on both the true bias (solid lines) and the estimated bias (dashed lines). So assuming the excitation is unknown and using the measured Fourier coefficients, we get a conservative error prediction.

Finally, we consider the bounds on $S_n(\omega)$. Again we use Shape No. 1, and we have the choice of using the a_m or the measured coefficients c_m. Requiring a frequency resolution of 0.1 Hz and expressing the bound width as a percentage of the upper bound, we obtain 1.2% with the exact coefficients and 3.8% with the measured coefficients. As before the measured coefficients give a conservative result.

We now have the necessary input parameters and a measure of their accuracy for use with the linear response relations. In

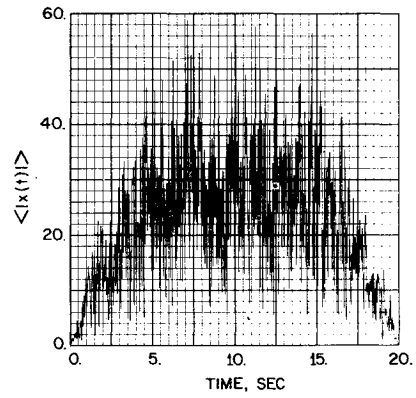

Fig. 11 Estimate of the first absolute moment of $x(t)$.

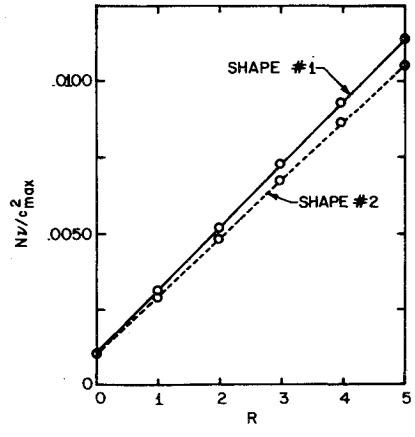

Fig. 13 Variability error vs R.

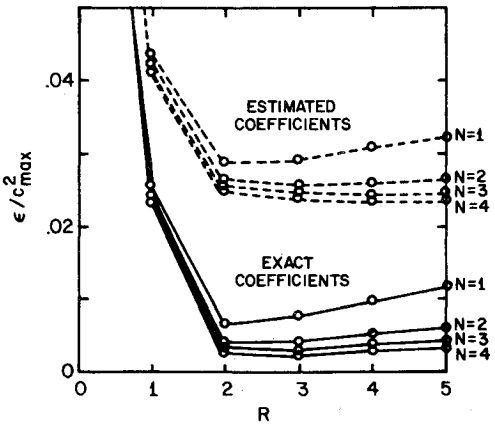

Fig. 14 Total error vs R.

this example, we can obtain reasonable accuracy for low orders of Fourier smoothing, and it is possible to obtain results without prior knowledge of the excitation process.

Conclusions

The integrated response analysis procedure presented here provides a convenient method for approximating time dependent spectral response of time invariant linear systems and determines necessary input parameters directly for experimental excitation records. It offers computational advantages over other techniques and allows accuracy to be adjusted as desired to minimize computational effort. No restrictions are placed on process or linear system bandwidth.

The data analysis procedure may be simpler and easier to apply than previously available techniques which require time-frequency filtering to obtain time dependent spectra or time pair analysis for autocorrelations, and it has the additional advantage of incorporating a measure of error in the estimation. This error is smallest for slowly varying envelope functions.

References

[1] Caughey, T. K. and Stumpf, H. J., "Transient Response of a Dynamic System Under Random Excitation," *Transactions of the ASME: Journal of Applied Mechanics,* Ser. E, Vol. 28, No. 4, Dec. 1961, pp. 563–566.

[2] Barnoski, R. L. and Maurer, J. R., "Mean-Square Response of Simple Mechanical Systems to Nonstationary Random Excitation," *Transactions of the ASME: Journal of Applied Mechanics,* Ser. E, Vol. 36, No. 2, June 1969, pp. 221–227.

[3] Bucciarelli, L. L. and Kuo, C., "Mean-Square Response of a Second-Order System to Nonstationary Random Excitation," *Transactions of the ASME: Journal of Applied Mechanics,* Ser. E, Vol. 37, No. 3, Sept. 1970, pp. 612–616.

[4] Verdon, J. M., "Response of a Single-Degree-of-Freedom System to Modulated White Noise," *Transactions of the ASME: Journal of Applied Mechanics,* Ser. E, Vol. 40, No. 1, March 1973, pp. 296–297.

[5] Page, C. H., "Instantaneous Power Spectra," *Journal of Applied Physics,* Vol. 23, No. 1, Jan. 1952, pp. 103–106.

[6] Priestley, M. B., "Evolutionary Spectra and Nonstationary Processes," *Journal of the Royal Statistical Society,* Ser. B, Vol. 27, No. 2, 1965, pp. 204–237.

[7] Priestley, M. B., "Power Spectral Analysis of Non-Stationary Random Processes," *Journal of Sound and Vibration,* Vol. 6, No. 1, 1967, pp. 86–97.

[8] Mark, W. D., "Spectral Analysis of the Convolution and Filtering of Non-Stationary Stochastic Processes," *Journal of Sound and Vibration,* Vol. 11, No. 1, 1970, pp. 19–63.

[9] Chakravorty, M. K., "Transient Spectral Analysis of Linear Elastic Structures and Equipment Under Random Excitation," Research Rept. R72-18, Structures Publication 340, April 1972, Dept. of Civil Engineering, MIT, Cambridge, Mass.

[10] Hammond, J. K., "On the Response of Single and Multidegree of Freedom Systems to Non-Stationary Random Excitations," *Journal of Sound and Vibration,* Vol. 7, No. 3, 1968, pp. 393–416.

[11] Roberts, J. B., "The Covariance Response of Linear Systems to Non-Stationary Random Excitation," *Journal of Sound and Vibration,* Vol. 14, No. 3, 1971, pp. 385–400.

[12] Roberts, J. B., "The Covariance Response of Linear Systems to Locally Stationary Random Excitation," *Journal of Sound and Vibration,* Vol. 17, No. 3, 1971, pp. 299–307.

[13] Shinozuka, M., "Random Processes with Evolutionary Power," *Journal of the Engineering Mechanics Division, American Society of Civil Engineers,* Vol. 96, No. EM-4, Aug. 1970, pp. 543–545.

[14] Corotis, R. B., "Time-Dependent Power Spectra and First Passage Probabilities," Research Rept. R70-78, Structures Publication 301, Dec. 1970, Dept. of Civil Engineering, MIT, Cambridge, Mass.

[15] Vanmarcke, E. H., "Parameters of the Spectral Density Function: Their Significance in the Time and Frequency Domains," Research Rept. R70-58, Structures Publication 302, Oct. 1970, Dept. of Civil Engineering, MIT, Cambridge, Mass.

[16] Vanmarcke, E. H., "Properties of Spectral Moments With Applications to Random Vibration," *Journal of the Engineering Mechanics Division, American Society of Civil Engineers,* Vol. 98, No. EM-2, April 1972, pp. 425–446.

[17] Roberts, J. B., "Smoothing of Mean Square Estimates from Non-Stationary Data," *Journal of Sound and Vibration,* Vol. 22, No. 4, 1972, pp. 419–428.

[18] Papoulis, A., *Probability, Random Variables, and Stochastic Processes,* McGraw-Hill, New York, 1965, p. 163.

[19] Davis, W. R., Jr., "Nonstationary Spectral Analysis for Linear Dynamic Systems," Sc.D. thesis, June 1973, MIT Cambridge, Mass.; TR 504, May 1973, MIT Lincoln Lab., Lexington, Mass.

[20] Hou, S., "Earthquake Simulation Models and Their Applications," Research Rept. R68-17, May 1968, Dept. of Civil Engineering, MIT, Cambridge, Mass.

[21] Howell, L. J., and Lin, Y. K., "Response of Flight Vehicles to Nonstationary Atmospheric Turbulence," *AIAA Journal,* Vol. 9, No. 11, Nov. 1971, pp. 2201–2207.